Kovove Mater. 48 2010 337–343
DOI: 10.4149/km_2010_6_337

Long-term microstructural stability of intermetallic Ti-46Al-8Ta alloy during ageing at temperatures of 700–800 °C

J. Lapin[1]*, T. Pelachová[1], H. Staneková[1], M. Dománková[2]

[1] *Institute of Materials and Machine Mechanics, Slovak Academy of Sciences, Račianska 75, 831 02 Bratislava, Slovak Republic*
[2] *Faculty of Material Sciences and Technology, Slovak Technical University, Paulínska 16, 917 24 Trnava, Slovak Republic*

Received 30 September 2010, received in revised form 5 November 2010, accepted 5 November 2010

Abstract

The lamellar $\alpha_2(Ti_3Al) + \gamma(TiAl)$ microstructure of intermetallic Ti-46Al-8Ta (at.%) alloy is unstable and transforms to $\alpha_2 + \gamma + \tau$ type at temperatures ranging from 700 to 800 °C during long-term ageing up to 10000 h. TEM observations and selected area diffraction patterns show that the ternary τ phase with $B8_2$ type structure (space group $P6_3/mmc$) is preferentially formed along the grain and lamellar colony boundaries. Volume fractions of the τ and γ phases increase with increasing ageing time at the expense of decreasing volume fraction of the α_2 phase at all ageing temperatures. The lattice parameters of the α_2 and γ phases change during ageing when compared with those of the as-received alloy. The ageing temperatures have no measurable effect on the lattice parameters of the coexisting α_2, γ and τ phases after ageing for 10000 h. The Vickers microhardness decreases reaching a minimum after ageing for about 500 h and then increases to peak values with increasing ageing time. The ageing time longer than 1500 h leads to a continuous softening of the alloy at all ageing temperatures.

K e y w o r d s: titanium aluminides, TiAl, phase identification, microstructure, diffraction

1. Introduction

Cast TiAl-based alloys represent an important class of high-temperature structural materials providing a unique set of physical and mechanical properties for the automotive engines, stationary gas turbines and aircraft engines. However, the formation of coarse-grained microstructures during solidification [1] and significant chemical inhomogeneities of the TiAl-based castings [2] deteriorate the already low ductility and poor damage tolerance at ambient temperature. Two main approaches are applied to refine coarse-grained structure of cast TiAl-based alloys: (i) alloying with minor additions, mainly with boron, which usually leads to the formation of long boride particles that can act as failure initiation sites [1, 3], and (ii) formation of highly faulted massive $\gamma_M(TiAl)$ through a diffusionless transformation initiated by cooling at required rate from single α phase field [4, 5]. Hu et al. [6] showed that elements such as Nb and Ta had low diffusion coefficients in both α (Ti-based solid solution with hexagonal crystal structure) and $\gamma(TiAl)$ phases, and favoured the massive transformation over the lamellar formation at low cooling rates. These elements partition between α and γ phases when forming the $\alpha + \gamma$ lamellar microstructure and this requirement for their diffusion slows down the lamellar transformation. Based on this concept, a new "airhardenable" Ti-46Al-8Ta (at.%) alloy requiring only air cooling from single α phase field to form massive γ_M was designed [7, 8] within the European integrated project IMPRESS [9]. This alloy shows promising castability, mechanical properties, and relatively large processing window to achieve $\alpha_2(Ti_3Al) + \gamma(TiAl)$ microstructure during heat treatments [8]. According to a ternary Ti-Al-Ta phase diagram thermodynamically modelled by Witusiewicz and published by Jiang et al. [8], two-phase $\alpha_2 + \gamma$ microstructure of the Ti-46Al-8Ta (at.%) alloy was predicted to be stable

*Corresponding author: tel.: +421 2 49268290; fax: +421 2 49268312; e-mail address: ummslapi@savba.sk

below 1050 °C. However, an experimental evidence of a new ternary τ phase was found by Lapin et al. [10, 11] in this alloy after ageing at 750 °C. Accordingly, the ternary Ti-Al-Ta phase diagram was recently re-evaluated taking into account occurrence of the τ phase [11]. According to the thermodynamic calculations, the microstructure of the Ti-46Al-8Ta (at.%) alloy is expected to transform to the equilibrium $\gamma + \tau$ type during long--term ageing below 870 °C. However, this calculated type of microstructure has not been proved experimentally yet. Hence, the study of long-term microstructural stability of this alloy at designed operating temperatures is of great practical interest.

The aim of the present work is to study the effect of long-term ageing on microstructural stability and microhardness of a cast Ti-46Al-8Ta (at.%) alloy at temperatures ranging from 700 to 800 °C. In addition, the effect of ageing for 10000 h on lattice parameters of coexisting phases is evaluated.

2. Experimental procedure

The studied Ti-46Al-8Ta (at.%) alloy was provided by ACCESS [12] in the form of centrifugally cast and heat treated cylindrical bars with a diameter of 13 mm and length of 120 mm. Heat treatments consisted of hot isostatic pressing (HIP) at an applied pressure of 200 MPa, temperature of 1260 °C for 4 h, which was followed by solution annealing at 1360 °C for 1 h and air cooling. The heat treatment was finalized by HIP ageing at an applied pressure of 150 MPa, temperature of 1260 °C for 2 h followed by cooling at a rate of 0.083 °C s^{-1}. The as-received bars were cut to cylindrical samples with a diameter of 13 mm and thickness of 5 mm and isothermally aged in air. Long-term ageing experiments were performed at three temperatures of 700, 750 and 800 °C for various times ranging from 100 to 10000 h in air. After each ageing step Vickers microhardness measurements were performed at an applied load of 0.49 N on polished and slightly etched surfaces. The microstructure evaluation was performed by optical microscopy (OM), scanning electron microscopy (SEM), backscattered scanning electron microscopy (BSEM), X-ray diffraction (XRD) analysis, transmission electron microscopy (TEM) and energy-dispersive X-ray (EDX) spectroscopy. Samples for OM and SEM observations were prepared using standard metallographic techniques and etched in a solution of 150 ml H_2O, 25 ml HNO_3 and 10 ml HF. TEM samples were mechanically thinned to a thickness of about 50 μm. The thinning continued in a solution of 300 ml CH_3OH, 175 ml 2-butanol and 30 ml $HClO_4$ at a temperature of –10 °C and voltage of 40 V using TenuPol-5 apparatus until the sample perforation. TEM observations were performed on JEOL 500 microscope operating at 200 kV. XRD analysis was carried out using Bruker D8 DISCOVER diffractometer equipped with X-ray tube with rotating Cu anode operating at 12 kW. All measurements were performed in parallel beam geometry with parabolic Goebel mirror in the primary beam. Diffraction patterns were measured within an angular range 20°–110° of 2θ with an exposition time of 6 s and step size of 0.01°. The obtained diffraction data were analysed quantitatively using program EVA 11.0. The further refinement of the patterns to identify the crystal lattice parameters of coexisting phases was performed using TOPAS 3.0. The instrumental line profile was determined from the measurements of polycrystalline texture of free corundum with sufficiently large crystallite size at the same angular range. Volume fractions of coexisting phases and size of lamellar colonies were determined from digitalized micrographs using a computer image analyser.

3. Results and discussion

3.1. Microstructure of as-received alloy

Figure 1a shows the typical fine grain microstructure of the as-received Ti-46Al-8Ta (at.%) alloy. The microstructure consists mostly of plate-like α_2 phase (bright grey contrast) which forms small lamellar colonies within the γ phase, as seen in Fig. 1b. As shown by Saage et al. [7], such "convoluted" type of microstructure is formed by precipitation of the α and/or α_2 phases on four equivalent {111} planes of the massively transformed γ_M during the second HIP-ing at 1260 °C and cooling from two phase $\alpha + \gamma$ field. Figure 2a shows the typical TEM micrograph of the lamellar $\alpha_2 + \gamma$ colonies. Selected area diffraction (SAD) patterns from this region indicate the well known Blackburn crystallographic orientation relationship between the coexisting α_2 and γ phases in the form:

$$(0001)_{\alpha_2} \parallel \{\bar{1}\bar{1}1\}_{\gamma} \text{ and } \langle 11\bar{2}0\rangle_{\alpha_2} \parallel \langle 1\bar{1}0]_{\gamma}.$$

Besides the continuous α_2 and γ lamellae, some single-phase α_2 and γ grains are found in the microstructure, as seen in Fig. 2b. Two phase $\alpha_2 + \gamma$ microstructure of the as-received alloy is also confirmed by XRD analysis shown in Fig. 3.

It should be noted that because of the convoluted microstructure of the studied alloy, the parameters usually used for microstructure quantification such as colony size, lath distance, etc. are difficult to assess. Therefore, the microstructure is characterized by volume fraction of coexisting phases and mean length of the α_2 laths measured from BSEM images such as that shown in Fig. 1b. For the as-received alloy with

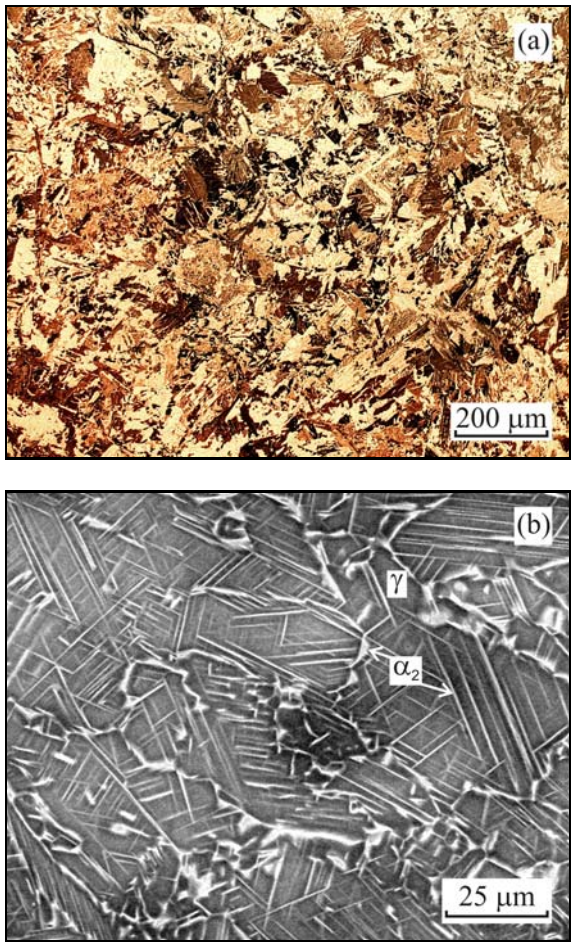

Fig. 1. (a) OM micrograph showing fine grain structure of the as-received Ti-46Al-8Ta (at.%) alloy. (b) BSEM micrograph showing the typical convoluted type of microstructure of the as-received alloy.

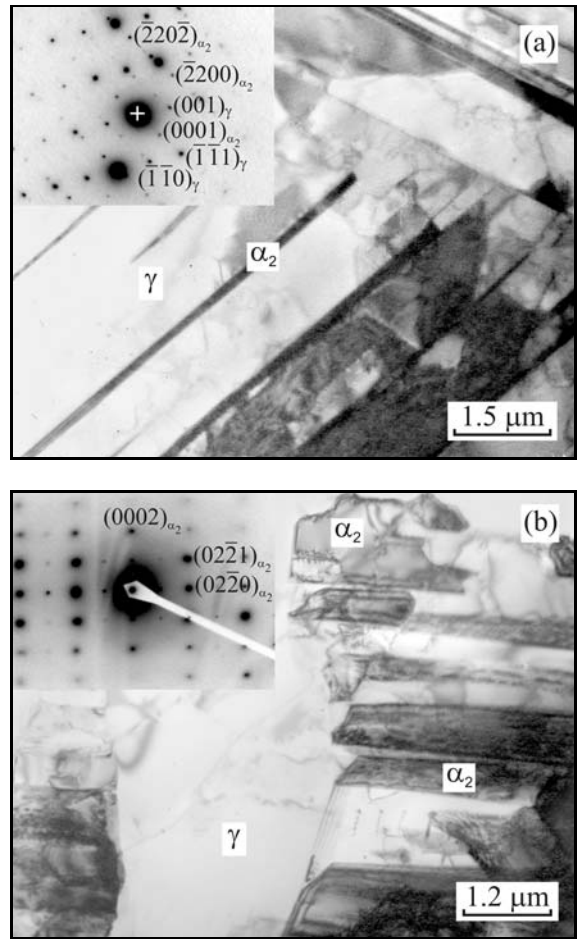

Fig. 2. TEM micrographs showing the microstructure of the alloy before ageing: (a) continuous α_2 and γ lamellae with corresponding SAD pattern from the zone axis $[1\bar{1}0]_{\gamma} \parallel [11\bar{2}0]_{\alpha_2}$; (b) single-phase α_2 and γ grains with corresponding SAD pattern from the zone axis $[2\bar{1}\bar{1}0]_{\alpha_2}$.

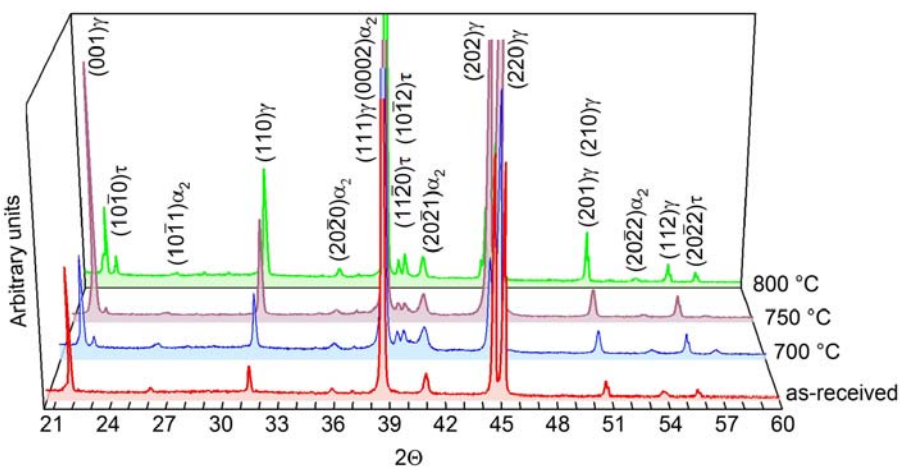

Fig. 3. X-ray diffraction patterns of the as-received alloy and after ageing for 10000 h. The ageing temperatures of 700, 750 and 800 °C are shown in the figure.

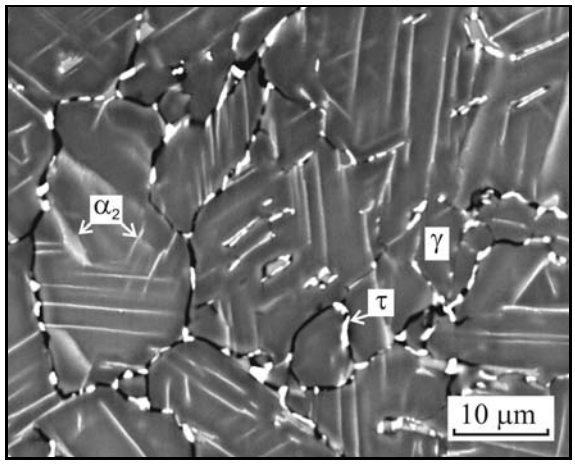

Fig. 4. BSEM micrograph showing the microstructure of the alloy after ageing at 750 °C for 10000 h.

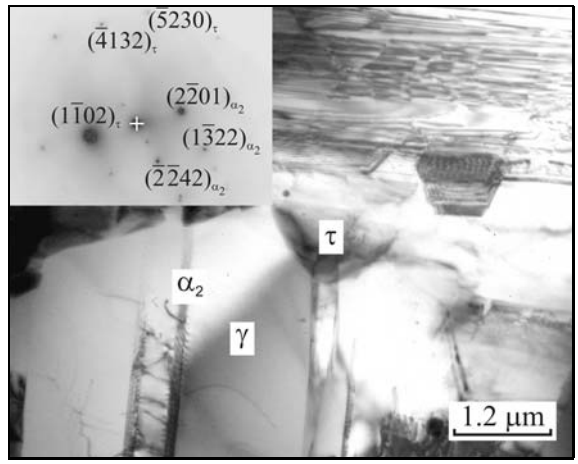

Fig. 5. TEM micrograph of the alloy aged for 2000 h with corresponding SAD pattern from the zone axis $[\bar{1}5\bar{4}12]_\tau \parallel [\bar{2}4\bar{2}9]_{\alpha_2}$.

the $\alpha_2 + \gamma$ microstructure, mean length and average volume fraction of the α_2 laths are measured to be (8.5 ± 0.3) μm and (29.8 ± 1.3) vol.%, respectively.

3.2. Effect of ageing on microstructure

Figure 4 shows the typical microstructure of the studied alloy after long-term ageing at the temperatures ranging from 700 to 800 °C. There are two main differences in the microstructure of the aged samples (Fig. 4) when compared to that of the as-received one (Fig. 1b): (i) precipitation of white colour phase particles predominantly at the grain and lamellar colony boundaries and (ii) the dark colour grain at colony boundaries clearly visible on BSEM images. The white colour particles with slightly varied chemical composition of Ti-(36-40)Al-(12-15)Ta (at.%) were identified recently by Lapin et al. [10, 11] to be a ternary τ phase with $B8_2$ type crystal structure (space group $P6_3/mmc$, Pearson symbol $hP6$) and Ni_2In symmetry [11]. The τ phase is similar to a ternary hexagonal Ti_4Al_3Nb phase reported by Witusiewicz et al. [13] for Ti-46Al-8Nb (at.%) alloy but is different from a binary $\sigma(Ta_2Al)$ phase with tetragonal crystal structure resulting from a ternary Ti-Al-Ta phase diagram proposed by Kubaschewski [14]. The lattice parameters a and c of the τ phase measured by XRD technique were found to increase and aspect ratio c/a decreased with increasing ageing time at 750 °C [11]. Figure 5 shows TEM micrograph of the τ phase formed at lamellar colony boundary in a sample aged at 750 °C for 2000 h. The τ phase can be clearly identified from SAD patterns using the measured lattice parameters determined by Lapin et al. [11], as illustrated by an insert of SAD pattern in Fig. 5. Besides the τ phase, the particles of the α_2 phase and Al enriched γ phase are also identified using EDX analysis and SAD patterns from the grain and colony boundaries.

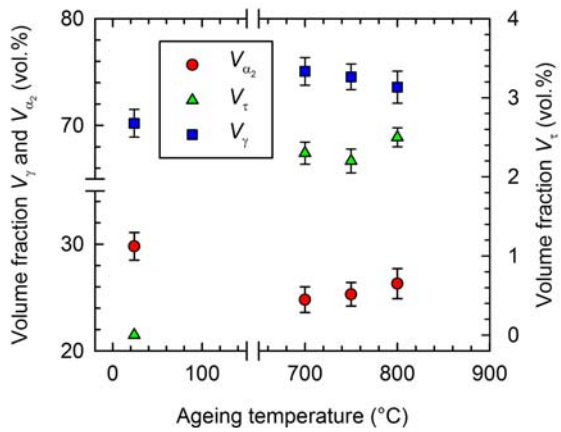

Fig. 6. Dependence of volume fraction of the γ (V_γ), α_2 (V_{α_2}) and τ (V_τ) phases on the ageing temperature after ageing for 10000 h.

XRD patterns shown in Fig. 3 clearly indicate that the $\alpha_2 + \gamma + \tau$ type of microstructure is preserved at all three ageing temperatures after long-term ageing for 10000 h. Figure 6 shows dependence of volume fraction of the coexisting α_2, γ and τ phases on the ageing time at three ageing temperatures. Increase of the ageing temperature and longer ageing time lead to an increase of the volume fractions V_τ and V_γ of the τ and γ phases, respectively, at the expense of a decrease of the volume fraction of the α_2 phase V_{α_2}. However, the ageing time as long as 10000 h is still insufficiently long to transform the initial $\alpha_2 + \gamma$ microstructure to the $\gamma + \tau$ type that is to be expected from the calculated phase diagram at temperatures below 870 °C [11].

The long-term ageing up to 10000 h has no measurable effect on fine grain structure of the studied al-

loy. A mean length of the α_2 laths within the lamellar colonies is measured to vary between (8.5 ± 0.3) μm and (9.2 ± 0.4) μm at all temperatures and ageing times.

3.3. Effect of ageing temperature on lattice parameters of coexisting phases

Figure 7 shows dependence of measured lattice parameters a and c of the γ, α_2 and τ phases on the ageing temperature for the samples aged for 10000 h. For the γ phase with an ordered $L1_0$ structure (space group P4/*mmm*), the lattice parameter a decreases and c increases after ageing at 700, 750 and 800 °C for 10000 h when compared with those for the as-received alloy. It should be noted that the lattice parameters of the as-received alloy are indicated at an ambient temperature in Fig. 7a. The ageing temperatures have no significant effect on the average values of a and c, which vary within the experimental error of the measurements. Since the microstructure of the studied alloy evolves from the massive γ_M, the measurements of lattice parameters of the γ_M phase have been also performed in the frame of this work on samples subjected to solution annealing at 1360 °C for 1 h and air cooling to room temperature. The quantitative analysis of X-ray diffraction data of such heat treated samples with the γ_M microstructure results in $a = (0.4033 \pm 0.0004)$ nm, $c = (0.4049 \pm 0.0004)$ nm and aspect ratio of $c/a = (1.0040 \pm 0.0002)$. The change of both the lattice parameters of the γ_M and γ phases during the precipitation of α/α_2 laths and subsequent long-term ageing (Fig. 7a) can be attributed to the redistribution of alloying elements, mainly to an increase of Al content in the γ phase [15–17].

For the α_2 phase with an ordered DO_{19} type structure (space group $P6_3/mmc$), both the lattice parameters a and c increase after ageing for 10000 h when compared to those measured in the as-received samples at an ambient temperature, as seen in Fig. 7b. On the other hand, the applied ageing temperatures have no effect on the average values of a and c, which vary within the experimental error of the measurements.

In the case of the τ phase with an ordered $B8_2$ type structure (space group $P6_3/mmc$), the lattice parameters a and c remain statistically the same after 10000 h ageing at the temperature range from 700 to 800 °C, as seen in Fig. 7c. It should be noted that both the lattice parameters of the τ phase increased with increasing ageing time up to 10000 h during ageing at 750 °C [11].

3.4. Effect of ageing time and temperature on Vickers microhardness

Figure 8 shows dependence of Vickers microhardness on the ageing time. At all three ageing temperatures, the Vickers microhardness first decreases with increasing ageing time reaching minimum values after the ageing for about 500 h and then increases to peak values after ageing for about 1500 h. The ageing time longer than 1500 h leads to softening of the alloy. The decrease of the Vickers microhardness at the early stages of ageing can be attributed to the recovery of an initial dislocation microstructure of the as-received

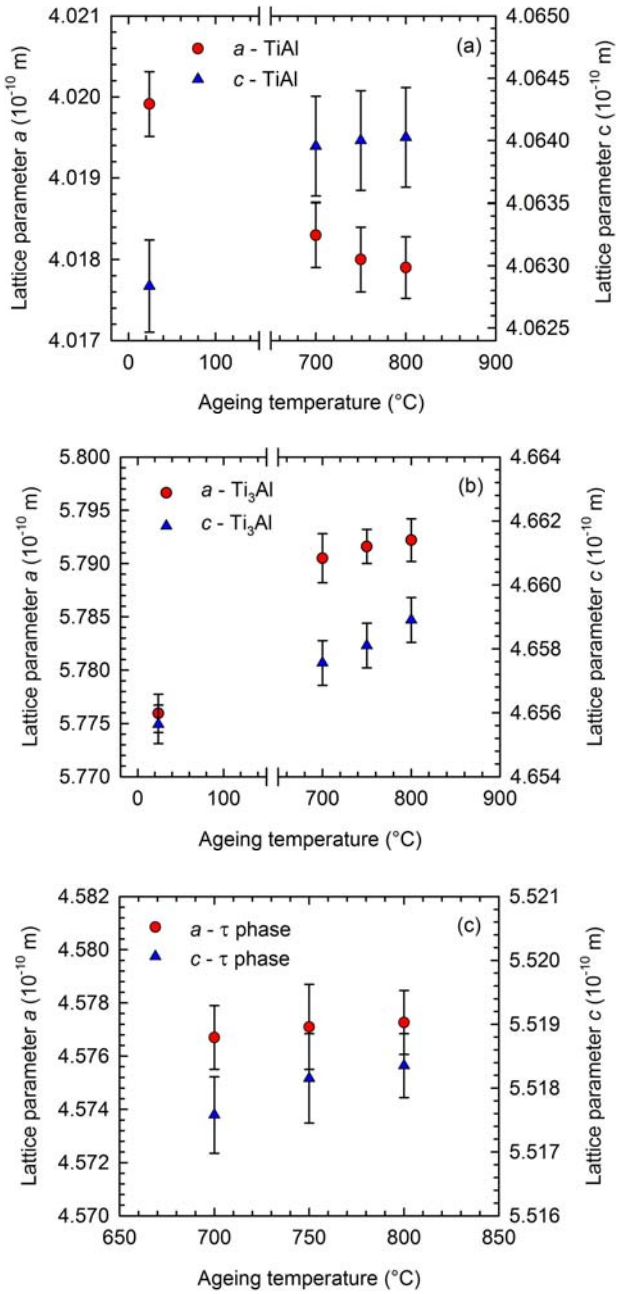

Fig. 7. Dependence of the lattice parameters a and c on the ageing temperature after ageing for 10000 h: (a) γ-TiAl, (b) α_2-Ti_3Al and (c) τ phase. The lattice parameters for the as-received alloy are shown at an ambient temperature.

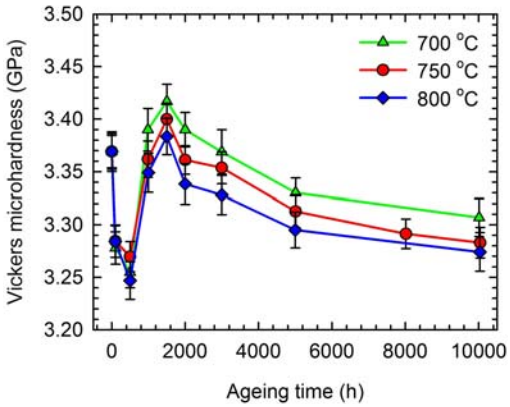

Fig. 8. Dependence of Vickers microhardness on the ageing time. The ageing temperatures are indicated in the figure.

material [18] and nucleation and early stages of growth of fine τ particles which is connected with a local depletion of elements contributing to the solid solution strengthening of the γ matrix. Further ageing is connected with the diffusion controlled growth of the α_2 and τ particles and redistribution of alloying elements within the γ matrix that lead to an increase of the microhardness. The softening process at the ageing times longer than about 1500 h can be attributed to a decrease of the volume fraction of the α_2 laths which is connected with a decrease of the contribution of the lamellar strengthening to overall measured microhardness. As shown by Lapin [19], the microhardness values can be related directly to offset yield stress of TiAl-based alloys with lamellar microstructure. Hence, the Vickers microhardness data shown in Fig. 8 can be considered as an indicative evolution of offset yield stress with the ageing time and temperatures for the studied alloy.

4. Conclusions

The investigation of long-term microstructural stability of Ti-46Al-8Ta (at.%) alloy during ageing at temperatures ranging from 700 to 800 °C suggests the following conclusions:

1. The lamellar $\alpha_2 + \gamma$ microstructure of the studied alloy is unstable and transforms to $\alpha_2 + \gamma + \tau$ type at all applied temperatures during long-term ageing up to 10000 h. Volume fraction of the τ and γ phases increases with increasing ageing time at the expense of decreasing volume fraction of the α_2 phase.

2. The lattice parameters of the α_2 and γ phases change during ageing when compared with those of the as-received alloy. The ageing temperatures have no measurable effect on the lattice parameters of the α_2, γ and τ phases after ageing for 10000 h.

3. The Vickers microhardness decreases with increasing ageing time reaching the minimum values after the ageing for about 500 h and then increases to peak values after ageing for about 1500 h. The ageing time longer than 1500 h leads to continuous softening of the alloy.

Acknowledgements

This work was financially supported by the Slovak Research and Development Agency under the contract APVV-0009-07 and EU Integrated Project IMPRESS "Intermetallic Materials Processing in Relation to Earth and Space Solidification" under the contract No. NMP3-CT-2004-500635. The authors would like to thank U. Hecht from ACCESS (Germany) for providing the experimental material and E. Dobročka from the Institute of Electrical Engineering of the Slovak Academy of Sciences for conducting XRD measurements.

References

[1] HECHT, U.—WITUSIEWICZ, V.—DREVERMANN, A.—ZOLLINGER, J.: Intermetallics, *16*, 2008, p. 969. doi:10.1016/j.intermet.2008.04.019

[2] ZOLLINGER, J.—GABALCOVÁ, Z.—DALOZ, D.—LAPIN, J.—COMBEAU, H.: Kovove Mater., *46*, 2008, p. 291.

[3] HU, D.—WU, X.—LORETTO, M. H.: Intermetallics, *13*, 2005, p. 914. doi:10.1016/j.intermet.2004.12.001

[4] HU, D.: Intermetallics, *9*, 2001, p. 1037. doi:10.1016/S0966-9795(01)00079-6

[5] CLEMENS, H.—BARTELS, A.—BYSTRZANOWSKI, S.—CHLADIL, H.—LEITNER, H.—DEHM, G.—GERLING, R.—SCHIMANSKY, F. P.: Intermetallics, *14*, 2006, p. 1380. doi:10.1016/j.intermet.2005.11.015

[6] HU, D.—HUANG, A. J.—WU, X.: Intermetallics, *15*, 2007, p. 327. doi:10.1016/j.intermet.2006.07.007

[7] SAAGE, H.—HUANG, A. J.—HU, D.—LORETTO, M. H.—WU, X.: Intermetallics, *17*, 2009, p. 32. doi:10.1016/j.intermet.2008.09.006

[8] JIANG, H.—ZHANG, K.—HAO, X. J.—SAAGE, H.—WAIN, N.—HU, D.—LORETTO, M. H.—WU, X.: Intermetallics, *18*, 2010, p. 938. doi:10.1016/j.intermet.2010.01.006

[9] JARVIS, D. J.—VOSS, D.: Mater. Sci. Eng. A, *413–414*, 2005, p. 583. doi:10.1016/j.msea.2005.09.066

[10] LAPIN, J.—GABALCOVÁ, Z.—PELACHOVÁ, T.—BAJANA, O.: Mater. Sci. Forum, *638–642*, 2010, p. 1368. doi:10.4028/www.scientific.net/MSF.638-642.1368

[11] LAPIN, J.—PELACHOVÁ, T.—WITUSIEWICZ, V. T.—DOBROČKA, E.: Intermetallics, *19*, 2011, p. 121. doi:10.1016/j.intermet.2010.09.016.

[12] AGUILAR, J.—HECHT, U.—SCHIEVENBUSCH, A.: Mater. Sci. Forum, *638–642*, 2010, p. 1275. doi:10.4028/www.scientific.net/MSF.638-642.1275

[13] WITUSIEWICZ, V. T.—BONDAR, A. A.—HECHT, U.—VELIKANOVA, T. Y.: J. Alloys Compd., *472*, 2009, p. 133. doi:10.1016/j.jallcom.2008.05.008

[14] KUBASCHEWSKI, O.: Aluminium-Tantalum-Titanium, Ternary Alloys. VCH 8. Materials Park, OH, ASM Alloy Phase Diagrams Center 1993, p. 406.
[15] PFULLMANN, T.—BEAVEN, P. A.: Scripta Metall. Mater., *28*, 1993, p. 275. doi:10.1016/0956-716X(93)90427-T
[16] KAWABATA, T.—FUKAI, H.—IZUMI, O.: Acta Mater., *46*, 1998, p. 2185. doi:10.1016/S1359-6454(97)00422-9
[17] PERDRIX, F.—TRICHET, M. F.—BONNENTIEN, J. L.—CORNET, M.—BIGOT, J.: Intermetallics, *9*, 2001, p. 807. doi:10.1016/S0966-9795(01)00066-8
[18] LAPIN, J.—PELACHOVÁ, T.—DOMÁNKOVÁ, M.: Intermetallics (submitted for publication).
[19] LAPIN, J.: J. Mater. Sci. Lett., *22*, 2003, p. 747. doi:10.1023/A:1023708110793